Proceedings of the Canadian Society for Mechanical Engineering International Congress
32nd Annual Conference of the Computational Fluid Dynamics Society of Canada
Canadian Society of Rheology Symposium
CSME/CFDSC/CSR 2025
May 25–28, 2025, Montréal, Québec, Canada

Deep Learning-Based Fatigue Detection Using Kinematic Information from Videos

Da Long[1], Sheng Yang[1*]

[1]School of Engineering, University of Guelph, Guelph, Canada
[*]Corresponding author: syang19@uoguelph.ca

***Abstract*—**Detecting human fatigue in manufacturing scenarios has been a long-standing research focus, driven by its profound impact on worker welfare. Fatigue contributes to work-related accidents and long-term musculoskeletal disorders, underscoring the need for effective monitoring solutions. With advancements in deep learning and image processing technologies, fatigue detection methods are increasingly adopting noninvasive approaches. Such solutions minimize disruptions to workers' activities while ensuring accurate monitoring. In this paper, we proposed a deep learning-based method that leverages motion and posture data extracted from videos to detect worker fatigue. This approach is both noninvasive and cost-effective, offering practical benefits for industrial applications.

***Keywords-component*—fatigue detection; deep learning; industrial applications; motion and posture analysis**

I. INTRODUCTION

Human involvement remains a critical component in modern manufacturing processes. A meta-analysis of studies on shift workers worldwide indicates that approximately 90% experience fatigue and sleepiness in the workplace [1]. In the United States, the economic impact of fatigue, both short-term and long-term, is estimated to cost employers $136 billion annually [2]. Consequently, the detection of human fatigue in manufacturing has garnered significant research attention. The advancements in deep neural networks (DNNs) have further accelerated progress, leading to notable innovation in this domain [3].

Among existing fatigue detection models, deep learning-based approaches have emerged as particularly advantageous [4]. Traditional methods, which rely on intricate mathematical modeling to account for the complexity of fatigue, often lack adaptability to individual variability and flexibility for diverse tasks. In contrast, deep learning methods effectively extract subtle fatigue patterns from high-dimensional data, such as sensor or camera outputs, while improving generalizability through dataset expansion [5].

Human fatigue in manufacturing settings encompasses both muscle and cognitive fatigue, both of which significantly influence posture change patterns and motion patterns [6], [7]. These patterns offer insights into fatigue from both biomechanical and behavioral perspectives. Continuous monitoring of kinematic metrics captures the cumulative nature of fatigue, while the diverse range of kinematic parameters provides a rich source of input for fatigue detection models [8].

The adoption of deep learning-based methods in fatigue detection is steadily increasing, yet relatively few studies focus on motion and posture change patterns [3]. Noninvasive detection is emerging as a dominant trend, as researchers aim to minimize disruptions to workers' operations [9]. However, most studies on motion and posture patterns rely on wearable sensors, such as inertial measurement units (IMUs), with only limited exploration of video-based approaches [23]–[25].

To bridge the gap in current fatigue detection research, this paper introduces a noninvasive deep learning approach that leverages motion and posture analysis from video inputs. The key novelties and contributions of the proposed work are as follows:

- We replace traditional wearable sensor-based approaches with computer vision techniques, enabling noninvasive kinematic analysis.
- A unique method is introduced that integrates motion and posture data as combined inputs.
- To address the cumulative nature of fatigue, a sequence-to-label training framework is proposed.
- This research pioneers a novel perspective by linking kinematic analysis to fatigue detection.

This paper is structured as follows: Section II provides an overview of related work. Section III outlines the methodology of the proposed method. Section IV examines the method's performance and discusses its limitations. Finally, Section V

concludes the paper.

II. Related Work

Fatigue detection, a key aspect of human factor (HF) modeling, plays a critical role in implementing effective fatigue management in manufacturing settings [10], [11]. Traditional methods typically construct mathematical models of fatigue levels by analyzing worker behaviors or physiological signals. However, the inherent complexity and variability of fatigue definitions make it challenging to establish a unified framework for quantifying fatigue [12]. As a result, traditional approaches often rely on idealized assumptions, such as controlled working environments or specific operation types, and struggle to handle high-dimensional and nonlinear data. In recent years, deep learning technologies have been extensively applied to fatigue-related data, yielding promising results [3]. Current deep learning-based approaches are generally categorized by data sources, including biosignal data, facial cues, and kinematic information.

A. Biosignals-Based Methods

Biosignals are generated by an organism's functional states and are expressed in various forms, including electrical, chemical, and optical signals. These signals provide valuable insights into physiological, mental, or pathological conditions and can be analyzed using specialized sensors or equipment [13].

Reference [14] utilized neural networks, both deep and shallow, to analyze electromyography (EMG) signals from the elbow to predict fatigue. Among the models tested, the Long Short-Term Memory (LSTM) network with Self-Attention (SA) achieved the best performance, surpassing traditional machine learning methods. In [15], researchers employed continuous wavelet transform and a convolutional neural network (CNN) to analyze electroencephalogram (EEG) data, achieving 88.5% accuracy in fatigue detection. In [16], researchers analyzed clinical electrocardiogram (ECG) data, performing feature selection before comparing the performance of various deep neural networks. Their results demonstrated that the LSTM with Consistency Self-Attention (CSA) yielded the highest accuracy. These studies highlight the sensitivity of biosignal-based deep neural networks in fatigue detection. However, even surface-contact sensors, such as surface EMG sensors, can interfere with participants' natural movement.

B. Facial-Cues-Based Methods

Facial cues, encompassing specific facial features or the overall facial description, play a critical role in fatigue detection methods, particularly in driver fatigue scenarios [17], [18]. In [19], researchers employed multi-block local binary patterns (MB-LBP) and an Adaboost classifier to identify facial key points, subsequently calculating the proportion of closed-eye time within a unit of time (PERCLOS) and yawning frequency. These metrics were then analyzed using fuzzy logic to determine driver fatigue. In [20], researchers used an enhanced YOLOv3-tiny convolutional neural network to identify facial regions, calculating closed-eye duration, blink frequency, and yawn frequency to estimate drivers' fatigue states, achieving an accuracy of 95.10%. In [21], researchers utilized 3D-CNN and bidirectional LSTM models to extract spatiotemporal features, outperforming traditional methods in yawning detection accuracy. While facial-cues-based methods are advantageous for achieving noninvasive fatigue detection, their robustness is limited due to individual variability, randomness in behavioral changes, and reliance on controlled experimental environments.

C. Kinematic-Information-Based Methods

Human kinematic data include body keypoint coordinates, velocities of keypoints, joint angles, and other metrics that collectively capture movement and posture changes [22]. In [23], researchers utilized Stacked Hourglass Networks to identify key joint points, integrated biomechanical calculations, and applied an existing fatigue mathematical model to detect fatigue in construction settings. In [24], researchers introduced a boundary-aware dual-stream MS-TCN algorithm to classify operation types and repetition counts, using a fatigue mathematical model to evaluate fatigue in human-robot collaboration (HRC) scenarios, improving task allocation. In [25], researchers applied an unsupervised Gaussian Mixture Model (GMM) clustering to analyze acceleration data from a motion capture suit for driver fatigue detection. Most kinematic information-based methods rely on sensor-derived data to recognize motion patterns and apply fatigue mathematical models. However, these methods are relatively complex compared to other approaches and still require participants to wear sensors.

The above methods have made notable progress in fatigue detection through deep learning techniques. While biosignal-based and facial-cues-based methods are more prevalent than kinematic-based approaches, they also exhibit greater diversity in model structures and input information, with a higher degree of deep neural network utilization. In contrast, kinematic-based methods often employ deep learning primarily for action recognition and rely heavily on mathematical models for fatigue assessment. However, biosignal-based methods are highly dependent on wearable or invasive sensors, and facial-cues-based methods focus more on detecting discrete events rather than continuous monitoring. Kinematic-based methods, by comparison, offer the potential of noninvasive and continuous monitoring of cumulative fatigue processes. With advances in computer vision, the development of a noninvasive, kinematic information-based approach leveraging deep learning techniques is necessary.

III. Methodology

Fig. 1 illustrates the overall framework of the proposed fatigue detection method, which comprises three modules. The first module is the wavelet transform module. This module processes an input video by employing computer vision techniques to extract key points from each frame, calculate selected feature values, and apply wavelet transform to these features. The output is a 2D matrix that encapsulates values for different

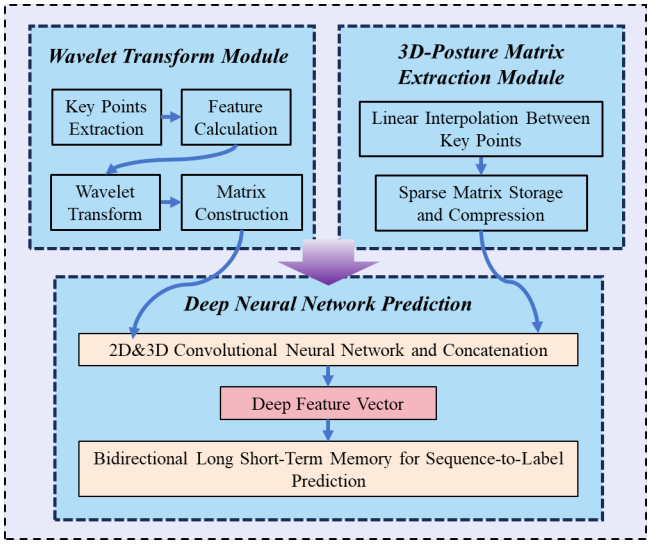

Figure. 1. Video-based fatigue detection framework

features across various wavelet transform layers. The second module, the 3D-posture extraction module, uses the key points from the first module to create a 3D matrix. The key points are mapped into the matrix, and linear interpolation is applied to define the skeleton within the 3D space. The resulting 3D matrix is then stored in sparse format. The third module, the deep neural network prediction module, integrates the outputs of the first two modules. A CNN processes the two matrices to produce a concatenated deep feature vector, which is then fed into a bidirectional LSTM (Bi-LSTM) using predefined sliding windows. The Bi-LSTM outputs a sequence label representing the fatigue level.

A. Wavelet Transform Module

To extract human motion patterns from video data, we developed a motion information extraction module based on wavelet transform. This module consists of two main components: the extraction of key points from video frames and the application of wavelet transform to the calculated features, generating a feature matrix for each frame. First, video frames were processed using OpenCV, and body key points were extracted using MediaPipe's pose estimation functionality [26], [27]. The processed video frames can be represented as: $F_i = \{(x_{i1}, y_{i1}, z_{i1}), \ldots, (x_{im}, y_{im}, z_{im})\}$, where m represents the number of key points on each frame.

In this study, we focused on assembly tasks in manufacturing scenarios, which predominantly involve upper limb movements. Therefore, the selected key points primarily represent the upper body, including the index finger, pinky finger, wrist, elbow, shoulder, and nose, totaling 11 key points. MediaPipe provides normalized x- and y-coordinates on the camera plane, as well as a predicted z-coordinate (depth information). To compute the required features, the normalized coordinates are converted into pixel coordinates:

$$x_{\text{pixel}} = x_{\text{norm}} \cdot W \tag{1}$$

$$y_{\text{pixel}} = y_{\text{norm}} \cdot H \tag{2}$$

$$z_{\text{pixel}} = z_{\text{norm}} \cdot D \tag{3}$$

The normalized coordinates are scaled by the width W, height H, and depth D of the video frame.

Monocular RGB cameras generally support frame rates of 30 fps or 60 fps. For this study, a frame rate of 30 fps was chosen, corresponding to the sampling frequency. Based on the time interval between consecutive frames, the following features are derived:

- **Velocity and Angular Velocity:** The linear velocity and angular velocity of key points in different directions.
- **Acceleration and Angular Acceleration:** The linear acceleration and angular acceleration of key points in different directions.
- **Joint Angles:** The angles formed by the shoulder, elbow, and wrist joints.
- **Forward Head Tilt Angle:** The angle between the plane formed by the nose and both shoulder key points and the camera plane, describing forward head tilt.
- **Lateral Head Tilt Angle:** The angles formed by the lines connecting the nose to each shoulder key point, representing lateral head tilt.

Additionally, variations in ambient lighting, camera instability, key point localization errors, and inaccuracies in depth prediction can introduce noise during the computation of the aforementioned features. To address this, as illustrated in Fig. 2, the Adjacent-Averaging algorithm was employed to smooth the calculated kinematic features, with reflective boundary conditions applied to enhance stability and accuracy [28].

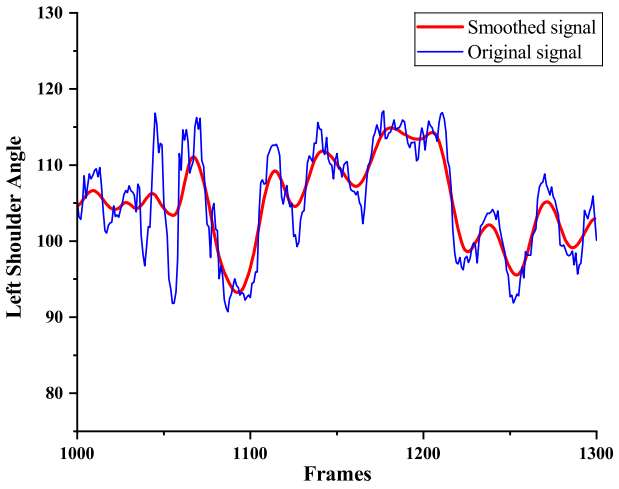

Figure. 2. The original and smoothed curves of the left shoulder joint angle

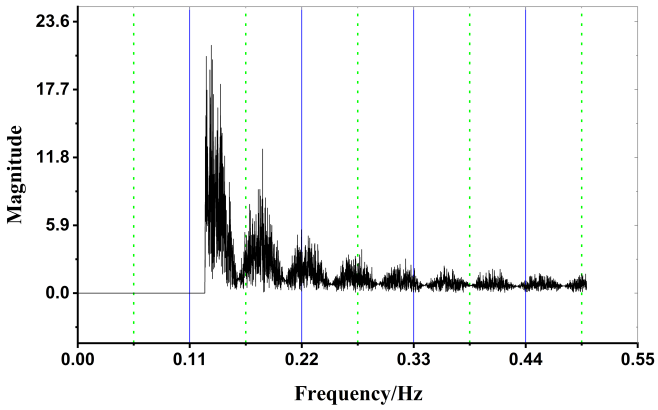

Figure. 3. Frequency components of the original signal for the left shoulder joint angle

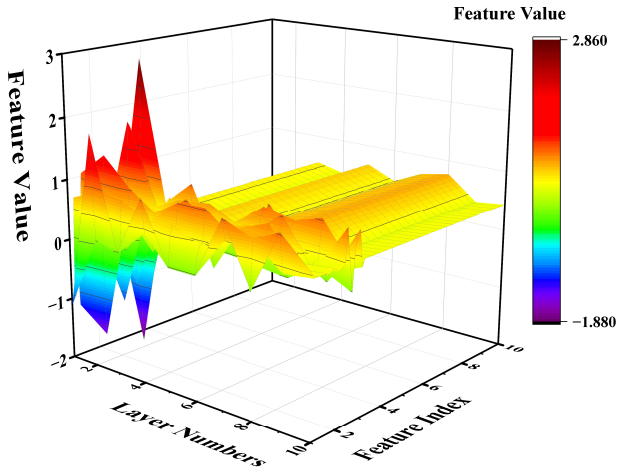

Figure. 4. Wavelet transform feature matrix

To ensure distortion-free sampling and facilitate further wavelet transformation, the Nyquist-Shannon sampling theorem must first be satisfied [29]:

$$f_s \geq 2 \cdot f_{\max} \tag{4}$$

The theorem ensures the sampling frequency (f_s) is at least twice the maximum signal frequency ($f_{\max}$) to prevent aliasing.

Fig. 3 depicts the frequency components of a specific feature derived using the Fast Fourier Transform (FFT) [30]. Frequency domain analysis of all features verified compliance with the Nyquist sampling theorem. Given the low-frequency and smooth nature of kinematic signals, the Daubechies discrete wavelet of length 8 was selected for decomposition and reconstruction [31]. The corresponding Daubechies wavelet function is defined as:

$$\psi(t) = \sum_{k=0}^{2N-1} (-1)^k c_{2N-1-k} \phi(2t-k) \tag{5}$$

where $\psi(t)$ is defined using the scaling function $\phi(t)$ and scaling coefficients c_k, with N denoting the number of vanishing moments.

Wavelet decomposition produces two sets of coefficients: approximation coefficients, which capture the signal's low-frequency components and overall trends, and detail coefficients, which represent its high-frequency components and rapid variations. Given the smooth and predominantly low-frequency characteristics of kinematic signals, the approximation coefficients from each decomposition level were used to reconstruct the signal through a multilevel process:

$$x(t) = \sum_{j=1}^{J} \text{Approximation\_Coeff}_j \cdot \phi_j(t) \tag{6}$$

Here, $\text{Approximation\_Coeff}_j$ are the approximation coefficients at level j, and $\phi_j(t)$ is the scaling function corresponding to level j. This series of reconstructions reflects the signal's components across different frequency levels. Consequently, it generates a sequence of matrices: $M = \{M_1, M_2, \ldots, M_k\}$, $M_i \in \mathbb{R}^{n \times l}$. Each matrix M_i has dimensions n (number of features) by l (number of wavelet transform levels), explaining kinematic information from multiple perspectives as shown in Fig. 4.

B. 3D-Posture Extraction Module

To incorporate positional information into the fatigue detection process, we developed a 3D posture extraction module. Initially, a blank matrix of dimensions $854 \times 480 \times 500$ was constructed, with all elements set to zero. Using the key points extracted from the first module, the matrix elements corresponding to the approximate locations of the key points (rounded coordinates) were set to 1. To represent the entire skeleton, linear interpolation was performed between key points:

$$P(t) = P_1 + t \cdot (P_2 - P_1), \quad t \in [0, 1] \tag{7}$$

Here, $P(t)$ is the interpolated point at parameter t, where t ranges from 0 to 1. P_1 corresponds to the starting key point, and P_2 corresponds to the ending key point. This process generated a sequence of matrices corresponding to the sequence of video frames, capturing the directional and positional information of the participant's limbs to form a position information stream, as shown in Fig. 5. However, due

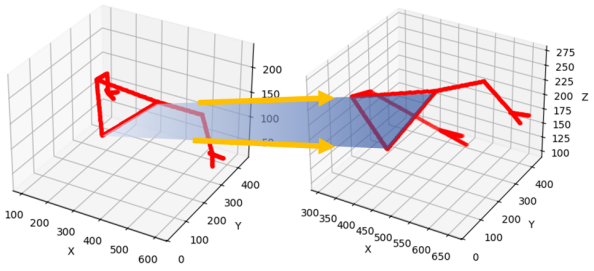

Figure. 5. 3D-posture matrix information flow

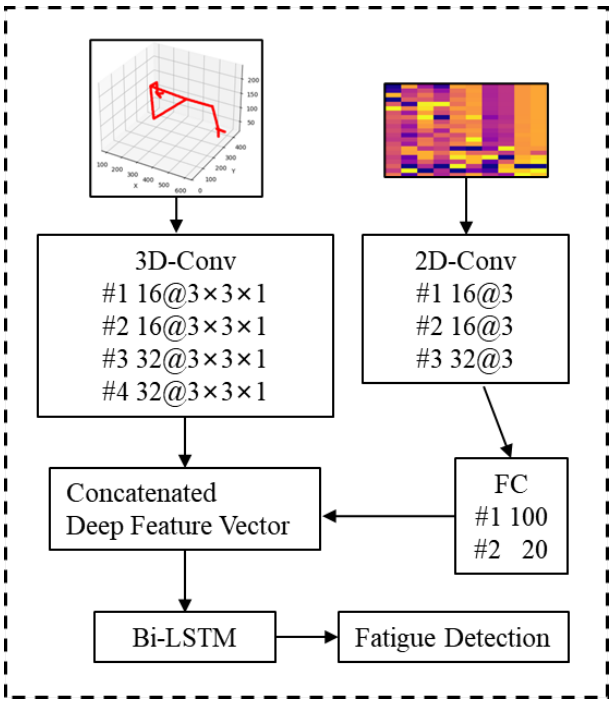

Figure. 6. Model architecture and hyperparameters

to the large initial matrix size, the matrices were cropped based on the average positions of the key points and subsequently downsampled, resulting in a final matrix size of $20 \times 20 \times 20$.

C. Model Structure and Training

As illustrated in Fig. 6, our CNN-LSTM model comprises two main components: a CNN-based deep feature extraction module and an LSTM-based sequence-to-label prediction module [32]. The input consists of two types of matrices extracted from the previously described modules, which are fed into the CNN. The CNN is employed due to its effectiveness in capturing detailed information from matrices [33]. For the 3D posture matrix, a 3D-CNN is used with four convolutional blocks (Conv Blocks) to extract a deep feature vector of length 20. The strides for these blocks are 1, 2, 3, and 3, respectively. For the wavelet transform matrix, a 2D-CNN is applied with three Conv Blocks, having strides of 1, 2, and 2, and a max-pooling layer added after the third Conv Block. This is followed by two fully connected layers to generate a deep feature vector of the same length.

Each Conv Block includes a convolutional layer, a batch normalization layer, a leaky ReLU layer to address the dying ReLU problem, and a dropout layer for regularization [34]. The convolutional layers use the kernel sizes and boundary paddings specified in Figure 5. The two deep feature vectors are concatenated and passed into the Bi-LSTM, with the last output serving as the summary label. The LSTM is particularly suited for this task because of its ability to model the sequential and accumulative nature of fatigue [35].

The hyperparameter tuning of the proposed model was guided by insights from related studies in time-sequential analysis and determined through empirical manual adjustments [36], [37]. The batch size was set to 32, with the model trained over 50 epochs using the Adaptive Moment Estimation (Adam) optimizer. The dynamic learning rate was initialized at 0.0001 and reduced by 90% after every 10 epochs. For all leaky ReLU layers, the slope scale was fixed at 0.1, and the dropout rate for each dropout layer was set to 30%. Given that LSTM models are more prone to overfitting compared to CNNs, the architecture included only a single LSTM layer with 50 hidden units. To mitigate overfitting, a dropout layer with a 30% dropout rate was added.

IV. Results and Discussion

To train and validate the proposed model, we utilized a custom video dataset. Three participants were instructed to perform two types of tasks: assembling a medicine bottle and assembling an air pump. As illustrated in Fig. 7, since only upper-body key points were used, the video recordings captured only the participants' upper bodies. Participants were then asked to self-report their perceived exertion using the Borg Rating of Perceived Exertion scale [38]. When the fatigue level reached 7 (indicating "very difficult"), the videos were segmented into fatigued and non-fatigued parts. Using a sliding window approach, frame sequences were divided with a window length of 450 frames (30 seconds) and a stride of 100 frames. The dataset was split into training, validation, and test sets in a ratio of 8:1:1. Additionally, to validate the use of Bi-LSTM, we conducted experiments using LSTM. The results showed that the CNN-Bi-LSTM model achieved an accuracy of 94.57%, compared to 88.57% for the CNN-LSTM model.

The results demonstrate the model's strong capability in analyzing motion and posture change patterns. However, the dataset lacks diversity in terms of participants and task types, which may limit its generalization ability. Furthermore, as a preliminary implementation, the experiment is designed for binary fatigue detection, whereas real-world fatigue levels are more complex. Future work will focus on expanding the dataset, developing more precise labeling mechanisms for fatigue levels, and reducing the overall complexity of the model.

V. Conclusion

This paper proposes a deep learning-based fatigue detection method that analyzes motion and posture change patterns from

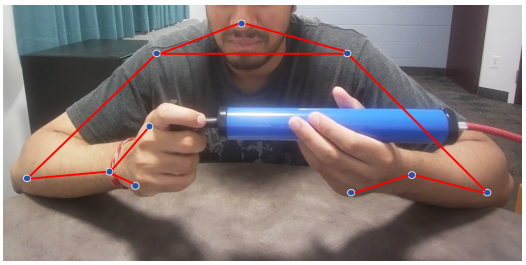

Figure. 7. The visualization of skeletal position prediction

video data, specifically targeting manufacturing scenarios. By utilizing neural networks to extract deep features that are more representative than traditional handcrafted features, the method achieves an accuracy of 94.57%. This work contributes to addressing gaps in kinematic information-based fatigue detection and offers a novel perspective for understanding the complex nature of fatigue.

VI. Acknowledgment

This research received financial support from the Social Sciences and Humanities Research Council (SSHRC) through the New Frontier Research Fund - Exploaration Grant (NFRFE-2022-00081).

References

[1] K. Richter, J. Acker, S. Adam, and G. Niklewski, "Prevention of fatigue and insomnia in shift workers—a review of non-pharmacological measures," EPMA journal, vol. 7, pp. 1–11, 2016.

[2] J. A. Ricci, E. Chee, A. L. Lorandeau, and J. Berger, "Fatigue in the US workforce: prevalence and implications for lost productive work time," Journal of occupational and environmental medicine, vol. 49, no. 1, pp. 1–10, 2007.

[3] R. Hooda, V. Joshi, and M. Shah, "A comprehensive review of approaches to detect fatigue using machine learning techniques," Chronic Diseases and Translational Medicine, 2021.

[4] S. A. El-Nabi, W. El-Shafai, E.-S. M. El-Rabaie, K. F. Ramadan, F. E. Abd El-Samie, and S. Mohsen, "Machine learning and deep learning techniques for driver fatigue and drowsiness detection: a review," Multimedia Tools and Applications, vol. 83, no. 3, pp. 9441–9477, 2024.

[5] S. Dara and P. Tumma, "Feature extraction by using deep learning: A survey," in 2018 Second international conference on electronics, communication and aerospace technology (ICECA), 2018, pp. 1795–1801.

[6] H. İ. Koruca, K. B. Urgancı, and S. C. Gamoura, "The Significance of Human Performance in Production Processes: An Extensive Review of Simulation-Integrated Techniques for Assessing Fatigue and Workload," in International Symposium on Intelligent Manufacturing and Service Systems, 2023, pp. 555–566.

[7] R. Terrier and N. Forestier, "Cognitive cost of motor reorganizations associated with muscular fatigue during a repetitive pointing task," Journal of Electromyography and Kinesiology, vol. 19, no. 6, pp. e487–e493, 2009.

[8] M. A. Al Imran, F. Nasirzadeh, and C. Karmakar, "Designing a practical fatigue detection system: A review on recent developments and challenges," Journal of Safety Research, vol. 90, pp. 100–114, 2024.

[9] N. Li et al., "Non-invasive Techniques for Muscle Fatigue Monitoring: A Comprehensive Survey," ACM Computing Surveys, vol. 56, no. 9, pp. 1–40, 2024.

[10] J. M. Finkelman, "A large database study of the factors associated with work-induced fatigue," Human factors, vol. 36, no. 2, pp. 232–243, 1994.

[11] A. Fletcher, B. Hooper, I. Dunican, and K. Kogi, "Fatigue management in safety-critical operations: History, terminology, management system frameworks, and industry challenges," Reviews of human factors and ergonomics, vol. 10, no. 1, pp. 6–28, 2015.

[12] N. Place and G. Y. Millet, "Quantification of neuromuscular fatigue: what do we do wrong and why?," Sports Medicine, vol. 50, no. 3, pp. 439–447, 2020.

[13] E. Kaniusas and E. Kaniusas, Physiological Phenomena and Biosignals. Springer, 2012.

[14] Y. Dang, Z. Liu, X. Yang, L. Ge, and S. Miao, "A fatigue assessment method based on attention mechanism and surface electromyography," Internet of Things and Cyber-Physical Systems, vol. 3, pp. 112–120, 2023.

[15] Y. Wang, Y. Huang, B. Gu, S. Cao, and D. Fang, "Identifying mental fatigue of construction workers using EEG and deep learning," Automation in Construction, vol. 151, p. 104887, 2023.

[16] Y. Bai, Y. Guan, and W.-F. Ng, "Fatigue assessment using ECG and actigraphy sensors," in Proceedings of the 2020 ACM International Symposium on Wearable Computers, 2020, pp. 12–16.

[17] G. Giannakakis et al., "Stress and anxiety detection using facial cues from videos," Biomedical Signal Processing and Control, vol. 31, pp. 89–101, 2017.

[18] G. Sikander and S. Anwar, "Driver fatigue detection systems: A review," IEEE Transactions on Intelligent Transportation Systems, vol. 20, no. 6, pp. 2339–2352, 2018.

[19] Z. Liu, Y. Peng, and W. Hu, "Driver fatigue detection based on deeply-learned facial expression representation," Journal of Visual Communication and Image Representation, vol. 71, p. 102723, 2020.

[20] K. Li, Y. Gong, and Z. Ren, "A fatigue driving detection algorithm based on facial multi-feature fusion," IEEE Access, vol. 8, pp. 101244–101259, 2020.

[21] H. Yang, L. Liu, W. Min, X. Yang, and X. Xiong, "Driver yawning detection based on subtle facial action recognition," IEEE Transactions on Multimedia, vol. 23, pp. 572–583, 2020.

[22] K.-N. An, "Kinematic analysis of human movement," Annals of biomedical engineering, vol. 12, pp. 585–597, 1984.

[23] Y. Yu, H. Li, X. Yang, L. Kong, X. Luo, and A. Y. Wong, "An automatic and non-invasive physical fatigue assessment method for construction workers," Automation in construction, vol. 103, pp. 1–12, 2019.

[24] H. Zheng, S. Chand, A. Keshvarparast, D. Battini, and Y. Lu, "Video-Based Fatigue Estimation for Human-Robot Task Allocation Optimisation," in 2023 IEEE 19th International Conference on Automation Science and Engineering (CASE), 2023, pp. 1–6.

[25] S. Ansari, H. Du, F. Naghdy, and D. Stirling, "Automatic driver cognitive fatigue detection based on upper body posture variations," Expert Systems with Applications, vol. 203, p. 117568, 2022.

[26] G. Bradski, "The OpenCV Library," Dr. Dobb's Journal of Software Tools, 2000.

[27] C. Lugaresi et al., "Mediapipe: A framework for building perception pipelines," arXiv preprint arXiv:1906.08172, 2019.

[28] A. Savitzky and M. J. Golay, "Smoothing and differentiation of data by simplified least squares procedures.," Analytical chemistry, vol. 36, no. 8, pp. 1627–1639, 1964.

[29] H. Nyquist, "Certain topics in telegraph transmission theory," Transactions of the American Institute of Electrical Engineers, vol. 47, no. 2, pp. 617–644, 1928.

[30] W. Cooley and J. W. Tukey, "An algorithm for the machine calculation of complex Fourier series," Mathematics of computation, vol. 19, no. 90, pp. 297–301, 1965.

[31] I. Daubechies, "Orthonormal bases of compactly supported wavelets," Communications on pure and applied mathematics, vol. 41, no. 7, pp. 909–996, 1988.

[32] M. Abadi et al., TensorFlow: Large-scale machine learning on heterogeneous systems. Mountain View, CA: Tensorflow, 2015.

[33] L. Alzubaidi et al., "Review of deep learning: concepts, CNN architectures, challenges, applications, future directions," Journal of big Data, vol. 8, pp. 1–74, 2021.

[34] L. Lu, Y. Shin, Y. Su, and G. E. Karniadakis, "Dying relu and initialization: Theory and numerical examples," arXiv preprint arXiv:1903.06733, 2019.

[35] R. C. Staudemeyer and E. R. Morris, "Understanding LSTM–a tutorial into long short-term memory recurrent neural networks," arXiv preprint arXiv:1909.09586, 2019.

[36] Y. Lu, H. Wang, B. Zhou, C. Wei, and S. Xu, "Continuous and simultaneous estimation of lower limb multi-joint angles from sEMG signals based on stacked convolutional and LSTM models," Expert Systems with Applications, vol. 203, p. 117340, 2022.

[37] T. Bao, S. A. R. Zaidi, S. Xie, P. Yang, and Z.-Q. Zhang, "A CNN-LSTM hybrid model for wrist kinematics estimation using surface electromyography," IEEE Transactions on Instrumentation and Measurement, vol. 70, pp. 1–9, 2020.

[38] N. Williams, "The Borg rating of perceived exertion (RPE) scale," Occupational medicine, vol. 67, no. 5, pp. 404–405, 2017.